Transcriptome Analysis of Skin Color Variation During and after Overwintering of Malaysian Red Tilapia

bingjie Jiang
Nanjing Agricultural University
lanmei Wang
Chinese Academy of Fishery Sciences Freshwater Fisheries Research Center
mingkun Luo
Chinese Academy of Fishery Sciences Freshwater Fisheries Research Center
jianjun Fu
Chinese Academy of Fishery Sciences Freshwater Fisheries Research Center
wenbin Zhu
Chinese Academy of Fishery Sciences Freshwater Fisheries Research Center
zaijie dong (dongzj@ffrc.cn)
Nanjing Agricultural University

Research Article

Keywords: red tilapia, skin color, transcriptome, overwintering, differentially expressed transcripts

Posted Date: July 27th, 2021

DOI: https://doi.org/10.21203/rs.3.rs-730510/v1

Version of Record: A version of this preprint was published at Fish Physiology and Biochemistry on April 13th, 2022. See the published version at https://doi.org/10.1007/s10695-022-01073-5.

Abstract

The commercial value of red tilapia is hampered by variations in skin color during overwintering. In this study, three types skin of red tilapia, including the skin remained pink color during and after overwintering (WP), the skin changed from pink color to black color during overwintering and remained black color after overwintering (PB), and the skin changed from pink color to black color during overwintering but recovered to pink color when the temperature rose after overwintering (BP), were used to analyze their molecular mechanisms of color variation. The transcriptome results revealed that the PB, WP, and BP libraries had 42, 43, and 43 million clean reads, respectively. The top 10 abundance mRNAs and specific mRNAs (specificity measure SPM > 0.9) were screened. After comparing intergroup gene expression levels, there were 2528, 1924 and 1939 differentially expressed genes (DEGs) between BP and PB, BP and WP, and PB and WP, respectively. Gene Ontology (GO) and Kyoto Encyclopedia of Genes and Genomes (KEGG) pathway analyses of color-related mRNAs showed that a number of DEGs, including *tyrp1*, *tyr*, *pmel*, *mitf*, *mc1r*, *asip*, *tat*, *hpdb* and *foxd3*, might play a potential role in pigmentation. Additionally, the co-expression patterns of genes were detected within the pigment-related pathways by PPI network from PB_WP group. Furthermore, DEGs from the apoptosis and autophagy pathways, such as *baxa*, *beclin1*, and *atg7*, might be involved in the fading of red tilapia melanocytes. The findings will aid in understanding the molecular mechanism underlying skin color variation in red tilapia during and after overwintering, as well as lay a foundation for future research aimed at improving red tilapia skin color characteristics.

Introduction

Tilapia is one of the excellent fish species recommended by the Food and Agriculture Organization of the United Nations (Gupta *et al.*, 2004). In recent years, tilapia has been widely accepted and has become an export dominant species of aquaculture in China (Pradeep et al., 2014). Red tilapia was obtained by crossing the mutant *Oreochromis mossambicus* with other tilapia populations such as *Oreochromis niloticus* and *Oreochromis aureus* (Li et al., 2003). Red tilapia is a valuable fish due to its uniform red skin, the absence of black peritoneum, very fast growth and adaptability to any culture system, and it has a huge market in many parts of the world, such as China, Malaysia and Thailand (Pradeep et al., 2014). Therefore, most studies on red tilapia have mainly focused on their growth and development in genetic breeding (Wardani et al., 2020; Zhu et al., 2016). However, the key issue restricting the growth of commercial red tilapia cultures is skin color variation during overwintering. Pavlidis et al. (2008) found that water temperature changed the body color by motility of chromatophore in red porgy (*Pagrus pagrus*), but the molecular mechanism for this change is unclear.

As one of the most diverse phenotypic characteristics in animals, coloration plays numerous adaptive functions such as camouflage, spouse choice, species identification, thermoregulation and photoreception (Hubbard et al., 2010). Furthermore, in aquaculture species, skin pigmentation pattern can be considered a factor of economic consideration. Therefore, skin colors might play a vital role in quality parameters in certain species. Previous studies have investigated that skin color was affected by many

factors, such as genetics, nutrition, physiology and environmental factors (Jiang et al., 2014; Luo et al., 2021). Water temperature is a major environmental factor for metabolism, development and growth of animals (Pavlidis et al., 2008). Many animals are dark under the cold and light under the warm condition (Kats *et al.*, 1986, Sherbrooke *et al.*, 1989). For example, both the dorsal and ventral skin colors of *Rana chiricahuensis* in low temperatures (5°C) were significantly darker than those exposed to 25°C (Fernandez *et al.*, 1991). *Pagrus* showed a darker dorsal skin area at low (15°C) water temperatures and lighter skin at 19°C (Pavlidis et al., 2008). The best pigmentation levels were achieved at temperatures from 26 to 30°C in goldfish (*Carassius auratus*) (Gouveia *et al.*, 2005). These researches are all focused on the physical or biochemical level. The molecular and cellular mechanisms of regulating skin color variation in fish, especially color variation during and after overwintering in red tilapia, are still unknown.

In our previous study, an Illumina RNA-seq and microRNA-seq analysis were conducted on different color varieties of red tilapia (Zhu et al., 2016; Wang et al., 2018). Wang et al. (2018) indicated that the color variation during overwintering period of red tilapia might be related to the changes of skin melanocytes and tyrosinase (TYR) activity. In our red tilapia breeding procedure, we found three kind changes of color, i.e. the skin remained pink color during and after overwintering (WP), the skin changed from pink color to black color during overwintering and remained black color after overwintering (PB), and the skin changed from pink color to black color during overwintering but recovered to pink color when the temperature rose after overwintering (BP). In this study, we used RNA-Seq to analyze the transcriptional profiles of WP, PB and BP skin color of red tilapia during and after overwintering. Particularly, we attempted to screen hundreds of differentially expressed genes (DEGs), which were responsible for skin color variation. Furthermore, the signaling pathways related to color variation during and after overwintering were also examined. Finally, several DEGs were validated by quantitative real-time polymerase chain reaction (qRT-PCR). This study will not only expose the molecular mechanism underlying red tilapia skin color variation during and after overwintering, but also provide valuable genetic information for breeding pure pink color tilapia.

Materials And Methods

Sample collection

The red tilapia used in this study was obtained from the pilot experimental station of Freshwater Fisheries Research Center (FFRC) affiliated with the Chinese Academy of Fishery Sciences. Whole pink red tilapia (initial weight: 500 ± 20 g) were cultivated in 2 mu plastic shed pond at the water temperatures of 18 ± 1℃ and fed twice a day (morning and evening) during the winter. In April of the next year, a few whole pink tilapias changed from pink color to black color. Then, the red tilapia with body color variation was cultured in the same environment without plastic shed, and the water temperature gradually rose with the ambient temperature. The red tilapia with reversible body color (black to pink) was selected.

Skin tissues were collected from four PB (pink changed to black) red tilapia, four WP (pink unchanged) red tilapia, and four BP (black return to pink) red tilapia individuals, respectively. All fresh tissue samples

were immediately snap-frozen in liquid nitrogen and then stored at − 80°C until use.

RNA extraction, cDNA library construction, and sequencing

Total RNA was obtained from red tilapia samples using RNA TRIzol (Invitrogen, UK) according to the manufacturer's protocol, and genomic DNA was removed using DNase (New England Biolabs). RNA purity was assessed using the Nanodrop-2000 (Thermo Scientific, USA). The ratio of A260:A280 in all RNA samples were higher than 1.9, and that of A260:A230 were higher than 1.8. Total RNA integrity was then subsequently checked using an Bioanalyzer RNA 6000 Pico Kit (Agilent Technologies). Samples with an RNA Integrity Number (RIN) > 8 were retained for subsequent analysis.

A total of twelve RNA samples of three different skin colors (four samples per skin color) were prepared and used for library construction. The libraries were constructed by TruSeq RNA Sample Prep Kit v2 (Illumina, San Diego, CA, USA) according to the manufacturer's instructions. Firstly, mRNA was purified from total RNA by Poly-T oligoattached magnetic beads, and then were fragmented under elevated temperature. Then first strand and second strand cDNA were subsequently synthesized. Secondly, the double stranded cDNA was purified for end repair, dA tailing, adaptor ligation, and DNA fragment enrichment. Finally, PCR was performed and aimed products were purified. The final product was assessed for its size distribution using Bioanalyzer DNA High Sensitivity Kit (Agilent Technologies). Each library was conducted on the Illumina X-Ten for 2×150 bp pair-end (PE) sequencing.

Quality control and Mapping to the reference genome

Quality of all raw reads was conducted by FastQC (Andrews 2014) software. At the initial filtering step, SOAPnuke (Chen et al., 2018) was used to discard poor quality reads, including adaptor reads and low-quality reads (reads with more than 50% bases with quality value less than 5). Then the clean reads were mapped onto reference genome independently by HISAT2 version 2.1.0 (Kim et al., 2015) with default values. And RSeQC packages (version 2.6.4) (Wang et al., 2012) were used to make a comprehensive evaluation on RNA-seq data after alignment, including sequencing saturation, mapped reads distribution, coverage uniformity, strand specificity, transcript level RNA integrity *etc*.

Differential expression analysis

Based on the HISAT2 alignment BAM file, featureCounts v1.6.2 (Liao et al., 2014) was used to estimate and quantify gene expression with default parameters, so as to generate the raw read count of each RNA genes. Gene expression was normalized by reads per kilobase of exon per million reads mapped (RPKM). Finally, edgeR (Robinson et al., 2010) was used to identify the DEGs by pairwise comparisons. The difference was considered significant if the $|\log FC| \geq 1$ and FDR (False Discovery Rate) ≤ 0.05.

To further understand the mRNA expression of each sample in red tilapia, the specificity measure (SPM) was introduced to analyze all screened mRNA (FPKM value ≥ 1, at least 3 samples) by PaGeFinder algorithms (Pan et al., 2012). SPM values greater than 0.9 were used as the selection criterion for specific genes. The higher the SPM value, the more the specific gene expression in the sample.

GO and KEGG enrichment analysis of differentially expressed genes

Gene Ontology (GO) term (http://www.geneontology.org/) enrichment and Kyoto Encyclopedia of Genes and Genomes (KEGG, http://www.kegg.jp/) enrichment analysis of DEGs were performed using clusterProfiler package (Yu et al., 2012), KOBAS v3.0 (Xie et al., 2011), respectively. The calculated *p*-value goes through Bonferroni Correction, taking *P*.adjust value ≤ 0.05 as a threshold.

Quantitative real-time PCR analysis

Total RNAs were extracted as described above. Each RNA sample was treated by 5× PrimeScript™ RT Master Mix (Takara) to remove residual genomic DNA and reverse transcribed into cDNA. All primer pairs (Additional file 1: Table S1) were designed based on the unigene sequences, and then synthesized by Sangon Biotech. (Shanghai, China). Real-time PCR was performed on a CFX-96 Real-time PCR System (Bio-Rad, CA, USA) in 25 μL reactions containing 12.5 μL SYBR Premix Ex Taq II (2×) (Takara Bio), 1 μL each primer (10 μM), 2 μL PCR template (cDNA) and 8.5 μL of nuclease-free water. Amplification was performed with an initial denaturation at 95°C for 5 min, followed by 40 cycles of 95°C for 10 s, 60°C for 30 s and 72°C for 30 s. All the reactions were conducted in triplicate, which six biological replicates. At the end of the PCR cycle, the relative expression was calculated using the $2^{-(\Delta\Delta Ct)}$ method with *β-actin* gene as the reference control. Data were analyzed statistically with SPSS 20 (IBM, Chicago, IL, USA) by t-test. Thresholds for statistical significance were set at $P<0.05$ (significant) and $P<0.01$ (highly significant).

Co-expression analysis of protein-protein interaction (PPI) network analysis

The DEGs were imported into the Search Tool for the Retrieval of Interacting Genes (STRING, https://string-db.org) database to obtain the PPI information (Szklarczyk et al., 2015). Only validated interactions with a composite score greater than 0.4 were considered significant. Cytoscape 3.6.0 software was used to construct PPI network and count the number of nodes in DEGs (Franz et al., 2016). The node genes with node degree above 10 were selected as the key target genes.

Results

Overview of the RNA-Seq data

To better understand skin color variation of red tilapia during and after overwintering, the mRNA libraries of PB, WP and BP were determined and analyzed by Illumina sequencing technology. In Table 1, we presented the Q30 percentage, GC percentage and the other indexes to describe the libraries. In total, an average of 42,721,496, 43,921,378 and 43,386,254 raw reads were obtained from the BP, PB and WP libraries, respectively. After filtering the low-quality reads and removing adaptor sequences, the average of 42,664,181, 43,888,258 and 43,347,484 clean reads were retrieved for further analysis. The percentage of G + C content and Q30 ratio was an average of 48.23% and 94.27%, indicated a high-quality sequence. All

raw transcriptome data were submitted to the NCBI Short Read Archive (SRA) database with the accession numbers PRJNA690595.

Table 1
The specific statistics for each library sequencing and quality control

Sample	Raw reads	Raw base(G)	Clean reads	Clean base(G)	Q30(%)	GC(%)
BP-1	40,313,772	6.05	40,254,280	6.00	95.23	48.31
BP-2	44,376,218	6.66	44,317,948	6.61	95.01	47.34
BP-3	40,589,108	6.09	40,530,756	6.05	95.01	47.84
BP-4	45,606,884	6.84	45,553,738	6.80	95.12	48.52
PB-1	46,324,834	6.95	46,289,448	6.88	93.32	47.41
PB-2	43,749,772	6.56	43,722,494	6.49	93.97	48.04
PB-3	40,425,896	6.06	40,402,734	5.98	93.81	48.37
PB-4	45,185,008	6.78	45,138,356	6.71	94.34	47.72
WP-1	43,218,496	6.48	43,170,434	6.42	93.80	49.02
WP-2	43,187,756	6.48	43,150,158	6.42	93.63	49.12
WP-3	43,362,090	6.50	43,324,748	6.46	93.92	48.15
WP-4	43,776,672	6.57	43,744,596	6.51	94.04	48.86
Average	43,343,042	6.50	43,299,974	6.44	94.27	48.23

To assess the quality of sequencing and reassembly, all clean reads were mapped to Nile tilapia (*Oreochromis niloticus*) genome within the range of known gene annotations. We found that 90.48%-94.62% of the clean reads could be mapped to the Nile tilapia reference genome (Additional file 1: Table S2). In particular, the percentage of multiple mapped reads and unique mapped reads for all libraries averaged 5.34% and 92.54%. In addition to consider the total mapping rate of sequencing reads and genomes for transcriptome sequencing, we also need to understand the distribution of mapped reads. The proportion of all reads operation in the CDs area exceeded 68.14%, and the ratio of matched with the intron area was the lowest, less than 8.71% (Additional file 1: Table S3).

Analysis of gene expression level of the red tilapia transcriptome

The RPKM method was used to estimate gene expression. The distribution of RPKM values for each sample were shown in Additional file 1: Table S4. A total of 33,437 genes were identified in the skin of red tilapia, and the expressed genes accounted for more than 63.26% of the total. The number of genes with $0 \leq RPKM \leq 1$ were the most, while the number of genes with $RPKM \geq 100$ were less than 1%.

Expression profiling of mRNAs

To further understand mRNA expression of differences skin colors in red tilapia, SPM analysis was conducted for each sample, in which the expressed mRNAs were filtered. 9755 mRNAs participated in SPM analysis with their mean RPKM value in each group, and 465 specific mRNAs were screened for the further analysis (SPM > 0.9, Additional file 2: Table S1). In detail, there were 119, 294, and 53 specific mRNAs in BP, PB, and WP skins respectively. The KEGG results of specific mRNAs showed that metabolic pathways, ribosome biogenesis in eukaryotes and oxidative phosphorylation were dominant pathway in BP skin and regulation of actin cytoskeleton, melanogenesis, tight junction and tyrosine metabolism were dominant in PB skin (Additional file 2: Table S2). Furthermore, we also analyzed the top 10 abundance mRNAs of differences skin color in red tilapia. As shown in Table 2, *Granulin* and *tat* gene were abundant from WP skin and other pigment-related genes were abundantly expressed in them, including *oca2* and *slc45a4*. *Tyrp1b* gene was the most abundant in PB skin and melanin synthesis gene accounts for the largest proportion of abundance expressed genes, such as *tyrp1b*, *pmelb*, *tyr*, *pmela*, and *tyrp1a*. In addition, *baxa* gene showed dominantly expression in BP skin.

Table 2
Ten most abundant genes of three difference colors in red tilapia during and after overwintering

WP	PB	BP
granulin	*tyrp1b*	*baxα*
tat	*cavin2a*	*si:ch73-86n18.1*
ENSONIG00000007142	*zgc:101810*	*crtac1a*
oca2	*pmelb*	ENSONIG00000040753
ENSONIG00000040391	*tyr*	*sdhb*
oni-mir-24a-4	*myh9a*	*ppdpfa*
col10a1a	ENSONIG00000019137	*loxa*
ENSONIG00000039537	*aqp3*	ENSONIG00000009288
slc45a4	*pmela*	ENSONIG00000018504
map3k7cl	*tyrp1a*	*atg7*

Differential gene expression (DEGs) identified in different skin patterns

In comparative transcriptome analysis, many genes showed different expression levels in three skin color samples. Under the criteria of FDR ≤ 0.05 and |logFC| ≥1, the volcano plots of three pairwise comparisons (BP_PB, BP_WP, and PB_WP) revealed the expression trend of each pair (Fig. 1a). We also constructed a histogram of DEGs in the three skin tissues (Fig. 1b). Compared with the PB skin, there were 2,528 DEGs in BP skin, of which 1,420 were up-regulated and 1,108 were down-regulated. A total of 1,091 DEGs were up-regulated in BP skin compared with WP skin, while 833 DEGs were down-regulated. There were 1,939 DEGs displaying greater abundance in PB skin compared with WP skin, of which 1,387 DEGs were up-regulated and 552 genes were down-regulated. Among these genes, 22 DEGs were detected as shared genes in each comparison group, in which 11 were known DEGs and seemed to play a key role in the color variation process (Fig. 2c). They were *st3gal1*, *si:ch73-86n18.1*, *plxna4*, *malb*, *fabp11a*, *plcb4*, *sdhb*, *si:dkey-65b12.6*, *si:ch211-157c3.4*, *agr1*, and *aqp3*, respectively.

To verify the credibility of the sequencing results, we randomly selected 25 DEGs related to pigment biosynthesis for qRT-PCR, including 13 up-regulated genes and 12 down-regulated genes. As shown in Fig. 2, the expression patterns of all down-regulated genes were consistent with the sequencing result, and 12 of the 13 up-regulated genes expression patterns were consistent with the sequencing results. The results showed that the reliability of the sequencing result was high.

Functional enrichment analysis of DEGs

The top GO function enrichment terms for the pairwise comparisons among three samples were shown in Additional file 2: Table S3. After GO annotation, all DEGs were classified into different biological processes, molecular function and cellular component. In each comparison, the top 50 of GO categories were selected in three different categories. The detailed annotations of each category were depicted in Additional file 1: Fig. S1a-c. In the molecular function category, binding and catalytic activity were the most mapped terms. In the biological process category, cellular process, metabolic process, biological regulation and regulation of biological process were the most mapped terms. In the cellular component category, cell, cell part, and membrane were the main mapped terms. Furthermore, a few DEGs were mapped to terms pigmentation-related terms such as developmental pigmentation (GO:0048066), melanocyte differentiation (GO:0030318), melanosome transport (GO: 0032402), retinal pigment epithelium development (GO:0003406) and pigmentation (GO:0043473). These genes enriched in pigmentation-related processes are informative and worthy a further study.

KEGG analysis of the pathways

To further explore the biological functions of the DEGs, an enrichment analysis based on KEGG database was performed. A total of 141 KEGG pathways were listed in this study (Additional file 2: Table S4). The DEGs between the BP and PB skins were involved in ribosome, oxidative phosphorylation, ribosome biogenesis in eukaryotes, cardiac muscle contraction, RNA degradation, RNA polymerase and DNA replication were significantly enriched ($P < 0.05$). The DEGs were significantly enriched in some genetic information processing between the BP and WP skins, including ribosome biogenesis in eukaryotes, spliceosome, RNA degradation and RNA polymerase. Ten pathways of oxidative phosphorylation,

ribosome biogenesis in eukaryotes, tight junction, adrenergic signaling in cardiomyocytes, cardiac muscle contraction, GNRH signaling pathway, mucin type o-glycan biosynthesis, sphingolipid metabolism, glycosphingolipid biosynthesis, taurine and hypotaurine metabolism were significantly enriched between the PB and WP skins ($P < 0.05$). Since fish skin color was mainly correlated with the synthesis of different pigments, we were interested in pigments biosynthesis pathway. Several pathways including oxidative phosphorylation, ribosome, Wnt (wingless-type MMTV integration site family) signaling pathway, MAPK (mitogen-activated protein kinase) signaling pathway, cell cycle, melanogenesis, tyrosine metabolism, autophagy pathway and apoptosis pathway, *etc.* were identified, which were related to the skin color regulation and pigmentation (Fig. 3).

Candidate genes related to melanophore

The KEGG pathway analysis results showed that 32 candidate genes were involved in pigmentation-related pathways, such as melanogenesis, tyrosine metabolism, Wnt signaling pathway and MAPK signaling pathway. These genes may play a potential role in skin color variation of red tilapia during and after overwintering. The heatmap of these genes (Fig. 4) indicated that four genes including agouti signaling protein (*asip*), tyrosine amino transferase (*tat*), hydroxyphenylpyruvate hydroxylase *(hpdb)* and forkhead transcription factor 3 (*foxd3*) were up-regulated in WP and BP group compared with the PB group, while the rest genes including tyrosinase (*tyr*), tyrosinase-related protein 1 (*tyrp1*), telanocortin receptor 1 (*mc1r*), microphthalmia-associated transcription factor (*mitf*), premelanosome protein (*pemel*) *etc*. were down-regulated in WP and BP group compared with PB group. In addition, some DEGs were involved in autophagy and apoptotic pathways such as *baxa*, *beclin1* and *atg7*. The expression of these genes in BP skin of red tilapia was significantly higher than that of PB skin, which play an important role in black-to-pink skin color transformation in red tilapia.

Correlation of candidate genes at protein levels

Based on the candidate genes in PB_WP groups, we identified the mutual correlation of their protein products using the STRING online tool (Fig. 5a). The genes (or proteins) from the pigmentation-related pathway were integrated together, and the relationship of them were extensive and strong. Among them, *asip*, *tat*, *hpdb*, *fox3* genes were significantly down-regulated, and other genes were significantly up-regulated. In addition, fourteen hub nodes in a PPI network with more than 10 nodes degree were shown in Fig. 5b. These hub genes included *tyr, mc1r*, *oca2*, *mitfb*, *slc45a2*, *tyrp1b*, *dct*, *asip*, *kit*, *kitlg*, *pmela*, *pmelb*, *mitfa*, *and egfra*. Among these genes, *tyr* gene showed the highest node degree, which was 18.

Discussion

To explore the different expression patterns among the three types skins, we performed differential gene expression analysis. When comparing PB skin to BP skin and WP skin, the results showed that more DEGs were up-regulated in PB skin, indicating that the formation of black skin is complex and that more genes are needed to participate in the process. Combined with the 10 abundance mRNAs result, there genes rich in melanin synthesis were abundantly expressed in PB skin, while a few of pigment genes were

abundantly expressed in WP. It was further suggested that melanin genes were involved in the body color variation of red tilapia during overwintering. Eleven known DEGs were shared by BP_PB, BP_WP and PB_WP comparison groups, of which *st3gal1*, *plxna4*, *fabp11a* and *aqp3* plays a vital role in regulating cell proliferation, migration and invasion (Wu et al., 2018; Wang et al., 2020). It has been reported that silencing of *st3gal1* gene suppresses melanoma invasion and significantly reduces the survive ability of aggressive melanoma cells of human in metastatic environment (Pietrobono et al., 2020). Plexins family can functionally activate tyrosine kinase receptors in mammalian, such as MET, RON, HER2, and KDR (Swiercz et al., 2008). Overexpression of *aqp3* gene can promoted the proliferation and migration of human hepatocytes (Chen et al., 2018). *Aqp3* can reduce the differentiation and inhibit the apoptosis of stem cells in human through reducing the expressions of related genes in Wnt/GSK-3 β/β-catenin pathway (Liu et al., 2020). *Fabp11a* were probably involved in cellular uptake and transport of fatty acids, targeting of fatty acids to transport systems and several signalling pathways in *Oryzias latipes* (Parmar et al., 2012). In this study, all of these genes expression suggested that skin color variation of red tilapia during overwintering might be related to the proliferation, migration and differentiation of melanocytes.

GO enrichment analysis of DEGs revealed that variations in pigmentation were related to cellular components and biological processes. Most of the DEGs clusters were consistent with previous works on fish, such as zebrafish (Higdon et al., 2013), Midas cichlids (*Amphilophus*) (Henning et al., 2013) and common carp (Li et al., 2015). KEGG pathway analysis showed that many DEGs were significantly enriched in oxidative phosphorylation, ribosome, ribosome biogenesis in eukaryotes and cardiac muscle contraction in the BP_PB group and PB_WP group. Several studies have shown that high expression of ribosomal protein related genes was associated with the black color in mice (Skarnes et al., 2011). Four of the five highly expressed genes in pigment cells of zebrafish were ribosomal protein (Higdon et al., 2013). There were many DEGs participate in oxidative phosphorylation, cardiac muscle contraction signal pathways in *Pristella maxillaris* (Bian *et al*., 2013) and *Lutjanus erythropterus* (Zhang et al., 2015). In addition, the KEGG results of specific mRNAs showed that ribosome biogenesis in eukaryotes, oxidative phosphorylation were dominant pathways in BP skin. Similar results were found in comparative analysis of BP_PB skin and PB_WP skin. It is suggested that these pathways may play an important role in color variation in red tilapia.

We also found that the DEGs of three skin colors of tilapia were mainly enriched in MAPK signaling pathway, Wnt signaling pathway, tyrosine metabolism, and melanogenesis. Tyrosinase metabolism and melanogenesis pathways have been reported in mammals. And both the Wnt and MAPK signaling pathways are involved in melanophore development in vertebrates (Fujimura et al., 2009, Zhang et al., 2017). For specific mRNA, the tyrosinase metabolism and melanogenesis pathways were dominant in PB skin. It showed that PB skin required more melanin synthesis than BP and WP skins. Meanwhile, we found that some DEGs between the BP and PB skin expressed abundantly in the process of apoptosis and autophagy pathways. The identification of genes in these pigmentation-related term and pathways are informative and are worthy of further study.

Studies have suggested that the mRNA expression levels of genes including *tyr*, *tyrp1*, *mc1r*, *mitf*, *pemel* were higher in PB skin. TYR carries out tyrosine hydroxylation to L-DOPA, which is the first step in the biosynthetic pathway of melanin. Under the action of dopachrome tautomerase (DCT) and TYRP1, the dopaquinone (DOPA) chrome was rapidly oxidized and polymerized to form melanin (Braasch et al. 2010, Simon et al., 2009). Therefore, TYR, TYRP1 and DCT are critical enzymes for the formation of melanin. Mutations or dysfunction of *tyr* or *tyrp1* genes lead to melanocyte death or extensive hypopigmentation in zebrafish (Krauss et al, 2015). In our study, compared to WP skin samples, the expression levels of *tyr* and *tyrp1* were the highest in PB skin. This was also consistent with the pigmentation of red crucian carp (Zhang et al, 2017). *Mitf* is a member transcription factor involved in the development of melanocytes, retinal cells, osteoclasts and mast cells (Minvielle et al., 2010). It has been reported that *mitf* could directly regulate the expression of multiple genes necessary for the development of melanophores, including *tyr*, *tyrp1*, and *dct* (Cheli et al., 2010). Compared with WP colors, PB skin color was caused by the increase of melanin content, suggesting that *mitf* may play a potential role in regulating the differentiation and development of melanocytes. *Mc1r* gene is a key gene in melanogenesis in animals. Alpha-melanocyte stimulating hormone (α-MSH) binds to *mc1r*, resulting in the decrease of cAMP level. Consequently, melanin biosynthesis process was triggered (Voisey et al., 2001). Previous studies have shown that *mc1r* mutations were associated with skin color variation in many fish species, such as cavefish, guppy, zebrafish and koi carp (Gross et al., 2009, Tezuka et al., 2011, Richardson *et al.*, 2008, Dong et al., 2020). Similarly, we observed a significant difference in *mc1r* expression between the red tilapia of three skin colors used in this study. *Pmel* gene acts as a scaffold in the melanosome by creating a proteolytic fibrillary matrix where melanin is deposited (Solano *et al.*, 2000). *Pmel* mutations promoted pigment dilution in many animals (Gutierrez et al., 2007). Here *pmel* was significantly up-regulated in PB skin when compared to WP and BP skin samples. Similarly, we observed the top 10 abundance mRNAs in PB skin, including *tyrp1b*, *tyr*, *pmelb*, *pmela*, *tyrp1a, etc.* All genes involved in melanin production, transport and structural proteins for melanin have been verified in red tilapia. In addition, we noticed that the proteins from pigment-related pathways were distinctly integrated together in PPI networks in PB_WP group. It was speculated that those proteins (or genes) could be co-regulated in skin color variation in red tilapia during overwintering. Among them, the most important top 10 genes based on the key nodes in the PPI network, including *tyr, mc1r*, *mitfb*, *tyrp1b*, *dct*, *pmela*, *pmelb*, and *mitfa*, *etc*, were consistent with the results of mRNA expression levels.

Regarding the black to pink stage, the mRNA expression levels of *asip*, *tat*, *hpdb* and *foxd3* were all up-regulated. *Asip* gene product blocks melanogenesis by antagonizing the binding of α-MSH to *mc1r. Asip* mutations were associated with skin color variation in Psetta maxima, zebrafish and medaka (Ceinos et al., 2015, Guillot et al., 2012, Jose´ et al., 2005). In our study, we observed higher expression of *asip* gene in BP skin transcripts and lower expression of *mc1r*, which further establishes the role of *asip* as an antagonistic of the *mc1r* gene. TAT and HPDB catalyze the substrate tyrosine to form homogeneous acid (HGA). Homogentisate1, 2-dioxygenase catalysis HGA to produce melatonin. Higher level of *tat* and *hpda* gene would directly reduce tyrosine level, thereby inhibited the synthesis of melanin (Zhang et al., 2008). In addition, *tat* gene was the most abundant in WP skin, suggested that it affected the skin variation in

red tilapia. *Foxd3* is a good candidate for the negative regulator of melanophore development. It can affect the lineage between neural or glial and pigment cells by repressing *mitf* at the early phase of neural crest migration (Thomas *et al.*, 2009). In addition, overexpression of *foxd3* in melb-a mouse melanoblasts blocked the expression of *mitf* (Lister et al., 2001). *Foxd3* was significantly up-regulated in BP skin samples compared to the PB skin, indicated that *foxd3* might play a significant role in the black-to-pink color transformation in red tilapia.

In addition, autophagy and apoptotic pathways were able to control the transition from black to pink in red tilapia. In detail, the mRNA level of apoptosis gene, such as *baxa*, was significantly increased in the body color transformation from the BP skin to the PB and WP skins. Meanwhile, the mRNA levels of *beclin1* and autophagy-related genes 7 (*atg7*), as the autophagy genes, were all upregulated in the BP skin compared with PB skin. *Baxa*, as one of the homologous proteins of BCL-2, could determine survival or death by an apoptotic stimulus. Overexpression of *baxa* may accelerate cell death (Oltvai et al., 1993). *Beclin1* plays a key role in regulating autophagy and cell death by interacts with either BCL-2 or PI3k class III (Takacs-Vellai et al., 2005). *Atg7* activates the ubiquitin-like protein ATGL2, which binds to *atg5* and extends the autophagic vesicle membrane. Whole body knock-out of *atg7* in mice led to death within 24h after birth (Komatsu et al., 2005). *Baxa* and *atg7* gene were among the top 10 abundance mRNAs in BP skin, further confirmed that appearance of autophagy may lead to melanocyte reduction.

Conclusions

In conclusion, we performed a transcriptome study of various skin colors during and after overwintering in red tilapia. We screened the top 10 abundance mRNAs, specific mRNAs and identified significant DEGs by pairwise comparison. These specifically expressed mRNAs provide the basis for further studies to clarify the role in skin variation of red tilapia. GO and KEGG analysis of specific mRNAs and DEGs identified numerous signaling pathways. We elucidated 32 candidate genes involved in skin color variation of red tilapia, and constructed a PPI network consist with these genes for revealing the mechanisms of color variation. These findings will help us learn more about the molecular mechanism of skin pigmentation in red tilapia. More specially, it provides valuable genetic data for breeding improved red tilapia strains with consistent skin color.

Declarations

Funding projects

This study was supported by the National Natural Science Foundation-Youth Fund Project (31802290).

Conflicts of interest/Competing interests

The authors have no relevant financial or non-financial interests to disclose.

Code availability

Not applicable

Availability of data and material

The authors declare that all other data supporting the findings of this study are available within the article and its supplementary information files.

Authors' contributions

Zaijie Dong conceived the study; Wenbin Zhu provided the experimental materials; Lanmei provided the funding for the experiment; Bingjie Jiang performed the experiments and wrote the paper; Jianjun Fu provided technical assistance in experiments; Mingkun Luo revised the manuscript; Zaijie Dong reviewed the manuscript; All authors read and approved the manuscript.

Ethics approval

The sampling scheme and experimental protocols were subject to approval by the Bioethical Committee of Freshwater Fisheries Research Center (FFRC) of the Chinese Academy of Fishery Sciences (CAFS) (BC 2013863, 9/2013). The methods of samples handled and experimental procedures carried out in accordance with the guidelines for the care and use of animals for scientific purposes issued by the Ministry of Science and Technology, Beijing China (No.398, 2006).

Availability of data and material/ Data availability

All data generated or analysed during this study are included in this published article (and its supplementary information files).

Consent to participate

Not applicable

Consent for publication

Not applicable

References

1. Andrews S (2014) FastQC: a quality control tool for high throughput sequence data. http://www.bioinformatics.babraham.ac.uk/projects/fastqc/
2. Bian FF, Yang XF, Ou ZJ et al (2019) Morphological characteristics and comparative transcriptome analysis of three different phenotypes of *Pristella maxillaris*. Front Genet 10:698
3. Braasch I, Liedtke D, Volff JN, Schartl M (2010) Pigmentary function and evolution of *tyrp1* gene duplicates in fish. Pigment Cell Melanoma Research 22(6):839–850
4. Ceinos RM, Guillot R, Kelsh RN et al (2015) Pigment patterns in adult fish result from superimposition of two largely independent pigmentation mechanisms. Pigment Cell Melanoma Research 28(2):196–209
5. Cheli Y, Ohanna M, Ballotti R, Bertolotto C (2010) Fifteen-year quest for microphthalmia-associated transcription factor target genes. Pigment Cell Melanoma Research 23(1):27–40
6. Chen G, Shi Y, Liu M, Sun J et al (2018) circHIPK3 regulates cell proliferation and migration by sponging miR-124 and regulating AQP3 expression in hepatocellular carcinoma. Cell Death Dis 9(2):175
7. Chen YX, Chen YS, Shi CM et al (2018) Soapnuke: a mapreduce acceleration supported software for integrated quality control and preprocessing of high-throughput sequencing data. Oxford Open 7(1):gix120
8. Dong ZJ, Luo MK, Wang LM et al (2020) MicroRNA-206 regulation of skin pigmentation in koi carp (*Cyprinus carpio* L.). Front Genet 11:47
9. Francisco S, María ME, Celia JC, Simon PH et al (2000) New insights on the structure of the mouse silver locus and on the function of the silver protein. Pigment Cell Melanoma Research 13(8):118–124
10. Franz M, Lopes CT, Huck G, Dong Y, Sumer O, Bader GD (2016) Cytoscape.Js a graph theory library for visualisation and analysis. Bioinformatics 32(2):309–311
11. Fujimura N, Taketo MM, Mori M et al (2009) Spatial and temporal regulation of Wnt/β-catenin signaling is essential for development of the retinal pigment epithelium. Dev Biol 334(1):31–45
12. Gouveia L, Rema P (2005) Effect of microalgal biomass concentration and temperature on ornamental goldfish (*Carassius auratus*) skin pigmentation. Aquac Nutr 11(1):19–23
13. Gross JB, Borowsky R, Tabin CJ (2009) A novel role for *mc1r* in the parallel evolution of depigmentation in independent populations of the cavefish *Astyanax Mexicanus*. Plos Genetics 5(1):1000326
14. Guillot R, Ceinos RM, Cal R et al (2012) Transient ectopic overexpression of agouti-signalling protein 1 (*asip1*) induces pigment anomalies in flatfish. Plos One 7(12):e48526
15. Gupta MV, Acosta BO (2004) A review of global tilapia farming practices. Aquaculture Asia 9(1):7–12
16. Gutierrez GB, Wiener P, Williams JL (2007) Genetic effects on coat color in cattle: dilution of eumelanin and´ phaeomelanin pigments in an F2-backcross *Charolais* × *Holstein* population. BMC Genet 8(1):56

17. Henning F, Jones JC, Franchini P et al (2013) Transcriptomics of morphological color change in polychromatic Midas cichlids. BMC Genom 14(1):171–171
18. Higdon CW, Mitra RD, Johnson SL et al (2013) Gene expression analysis of zebrafish melanocytes, iridophores, and retinal pigmented epithelium reveals indicators of biological function and developmental origin. Plos One 8(7):e67801
19. Huang R, Kitajama C, Ke C (1997) A Study on Induced factor of White Skin of Flat Fish *Paralichthys Olivaceus* (Temminck et Schlegel). Modern Fisheries Information 4(9):21–23
20. Hubbard JK, Uy JA, Hauber ME, Hoekstra HE, Safran RJ (2010) Vertebrate pigmentation: from underlying genes to adaptive function. Trends Genet 26:231–239
21. Jennifer R, Pia RL, Natalie LR, Julia RD et al (2008) *Mc1r* Pathway regulation of zebrafish melanosome dispersion. Zebrafish 5(4):289–295
22. Jiang YL, Zhang SH, Xu J et al (2014) Comparative transcriptome analysis reveals the genetic basis of skin color variation in common carp. Plos One 9(9):e108200
23. Jose´ MCR, Tatjana H, Helgi BS, Richard EP (2005) Gene structure of the goldfish agouti-signaling protein: a putative role in the dorsal-ventral pigment pattern of fish. Endocrinology 146(3):1597–1610
24. Kim D, Langmead B, Salzberg SL (2015) Hisat: a fast spliced aligner with low memory requirements. Nature methods 12(4):357–360
25. Komatsu M, Waguri S, Ueno T et al (2005) Impairment of starvation-induced and constitutive autophagy in *atg7* deficient mice. J Cell Biol 169(3):425–434
26. Krauss J, Geiger-Rudolph S, Koch I, Nusslein-Volhard C, Irion U (2015) A dominant mutation in *tyrp1a* leads to melanophore death in zebrafish. Pigm Cell Melanoma Research 27(5):827–830
27. Li XJ, Li SF, Feng JH et al (2003) Preliminary study on salinity tolerance of Israel red tilapia. Journal of Shanghai Fisheries University 12(3):205–208
28. Li XM, Song YN, Xiao GB, Zhu BH, Xu GC, Sun MY et al (2015) Gene expression variations of red-white skin coloration in common carp (*Cyprinus carpio*). Int J Mol Sci 16:21310–21329
29. Liao Y, Gordon K, Smyth, Shi W (2014) Featurecounts: an efficient general purpose program for assigning sequence reads to genomic features. Bioinformatics 30(7):923–930
30. Lister JA, Close J, Raible DW (2001) Duplicate *mitf* genes in zebrafish: complementary expression and conservation of melanogenic potential. Dev Biol 237(2):333–344
31. Liu CS, Liu LY, Zhang Y, Jing HY (2020) Molecular mechanism of *aqp3* in regulating differentiation and apoptosis of lung cancer stem cells through Wnt/GSK-3β/β-Catenin pathway. Jbuon 25(4):1714–1720
32. Luo MK, Lu GQ, Yin HR et al (2021) Fish pigmentation and coloration: molecular mechanisms and aquaculture perspectives. Reviews in Aquaculture 00:1–18
33. Minvielle F, Bed'Hom B, Coville JL et al (2010) The "silver" Japanese quail and the *mitf* gene: causal mutation, associated traits and homology with the "blue" chicken plumage. BMC Genet 11(1):1–7

34. Nakano T, Ono K, Takeuchi M (1992) Levels of zinc, iron, and cupper in the skin of abnormal pigmented Japanese flounder. Nippon Suisan Gakkaishi 58(11):2207
35. Oltvai ZN, Milliman CL, Korsmeyer SJ (1993) Bcl-2 heterodimerizes in vivo with a conserved homolog, *bax*, that accelerates programed cell death. Cell 74(4):609–619
36. Pan JB, Hu SC, Wang H et al (2012) PaGeFinder: quantitative identification of spatiotemporal pattern genes. Bioinformatics 28(11):1544–1545
37. Parmar MB, Venkatachalam AB, Wright JM (2012) The evolutionary relationship of the transcriptionally active *fabp11a* (intronless) and *fabp11b* genes of medaka with *fabp11* genes of other teleost fishes. Febs Journal 279(13):2310–2321
38. Pavlidis M, Karkana M, Fanouraki E et al (2008) Environmental control of skin color in the red porgy, *Pagrus pagrus*. Aquac Res 39(8):837–849
39. Pietrobono S, Anichini G, Sala C et al (2020) ST3GAL1 is a target of the SOX2-GLI1 transcriptional complex and promotes melanoma metastasis through AXL. Nat Commun 11(1):5865
40. Pradeep PJ, Srijaya TC, Hassan A et al (2014) Optimal conditions for cold-shock induction of triploidy in red tilapia. Aquacult Int 22(3):1163–1174
41. Robinson MD, Mccarthy DJ, Smyth GK (2010) Edger: a bioconductor package for differential expression analysis of digital gene expression data. Bioinformatics 26(1):139–140
42. Simon DJ, Peles D, Wakamatsu K, Ito S (2009) Current challenges in understanding melanogenesis: bridging chemistry, biological control, morphology and function. Pigment Cell Melanoma Research 22(5):563–579
43. Skarnes WC, Rosen B, West AP et al (2011) A conditional knockout resource for the genome-wide study of mouse gene function. Nature 474(7351):337–342
44. Swiercz JM, Worzfeld T, Offermanns S (2008) ErbB-2 and met reciprocally regulate cellular signaling via plexin-B1. J Biol Chem 283(4):1893–1901
45. Szklarczyk D, Franceschini A, Wyder S et al (2015) STRING v10: protein-protein networks, integrated over the tree of life. Nucleic Acids Res 43:D447–D452
46. Takacs-Vellai K, Vellai T, Puoti A, Passannante M et al (2005) Inactivation of the autophagy gene *bec-1* triggers apoptotic cell death in *C. elegans*. Curr Biol 15(16):1513–1517
47. Tezuka A, Yamamoto H, Yokoyama J et al (2011) The *mc1r* gene in the guppy (*Poecilia reticulata*): Genotypic and phenotypic polymorphisms. BMC Research Notes 4(1):31
48. Thomas AJ, Erickson CA (2009) *Foxd3* regulates the lineage switch between neural crest-derived glial cells and pigment cells by repressing *mitf* through a non-canonical mechanism. Development 136(11):1849–1858
49. Voisey J, Box NF, Daal AV (2001) A polymorphism study of the human agouti gene and its association with *mc1r*. Pigment Cell Res 14(4):264–267
50. Wang LG, Wang SQ, Li W (2012) RSeQC: quality control of RNA-seq experiments. Bioinformatics 28(16):2184–2185

51. Wang LM, Song FB, Zhu WB et al (2018) Effects of temperature on body color of Malaysian red tilapia during overwintering period. Journal of Fisheries of China 42(1):72–79
52. Wang XY, Yang J, Yao Y, Shi X, Yang GS, Li X (2020) *Aqp3* facilitates proliferation and adipogenic differentiation of porcine intramuscular adipocytes. Genes 11(4):453
53. Wardani WW, Alimuddin A, Junior MZ et al (2020) Growth performance, robustness against stress, serum insulin, *igf-1* and *glut4* gene expression of red tilapia (*Oreochromis sp.*) fed diet containing graded levels of creatine. Aquaculture Nutrition 27(1):274–286
54. Wu X, Zhao JD, Ruan YY et al (2018) Sialyltransferase *st3gal1* promotes cell migration, invasion, and TGF-β1-induced EMT and confers paclitaxel resistance in ovarian cancer. Cell Death Dis 9(11):1102
55. Xie C, Mao XZ, Huang JJ, Yang D et al (2011) KOBAS 2.0: a web server for annotation and identification of enriched pathways and diseases. Nucleic Acids Res 39(suppl_2):W316–W322
56. Yu GC, Wang LG, Han YY, He QY (2012) Clusterprofiler: an r package for comparing biological themes among gene clusters. Omics-a Journal of Integrative Biology 16(5):284–287
57. Zhang Y, Wang L, Zhang S, Yang H, Tan H (2008) HmgA, transcriptionally activated by *hpda*, influences the biosynthesis of actinorhodin in *Streptomyces Coelicolor*. FEMS Microbiol Lett 280(2):219–225
58. Zhang YP, Wang ZD, Guo YS et al (2015) Morphological characters and transcriptome profiles associated with black skin and red skin in crimson snapper (*Lutjanus erythropterus*). Int J Mol Sci 16(11):26991–27004
59. Zhang YQ, Jin H et al (2017) Comparative transcriptome analysis of molecular mechanism underlying gray-to-red body color formation in red crucian carp (*Carassius auratus*, red var.). Fish Physiol Biochem 43(6):1387–1398
60. Zhu WB, Wang LM, Dong ZJ et al (2016) Comparative transcriptome analysis identifies candidate genes related to skin color differentiation in red tilapia. Sci Rep 6(1):31347

Figures

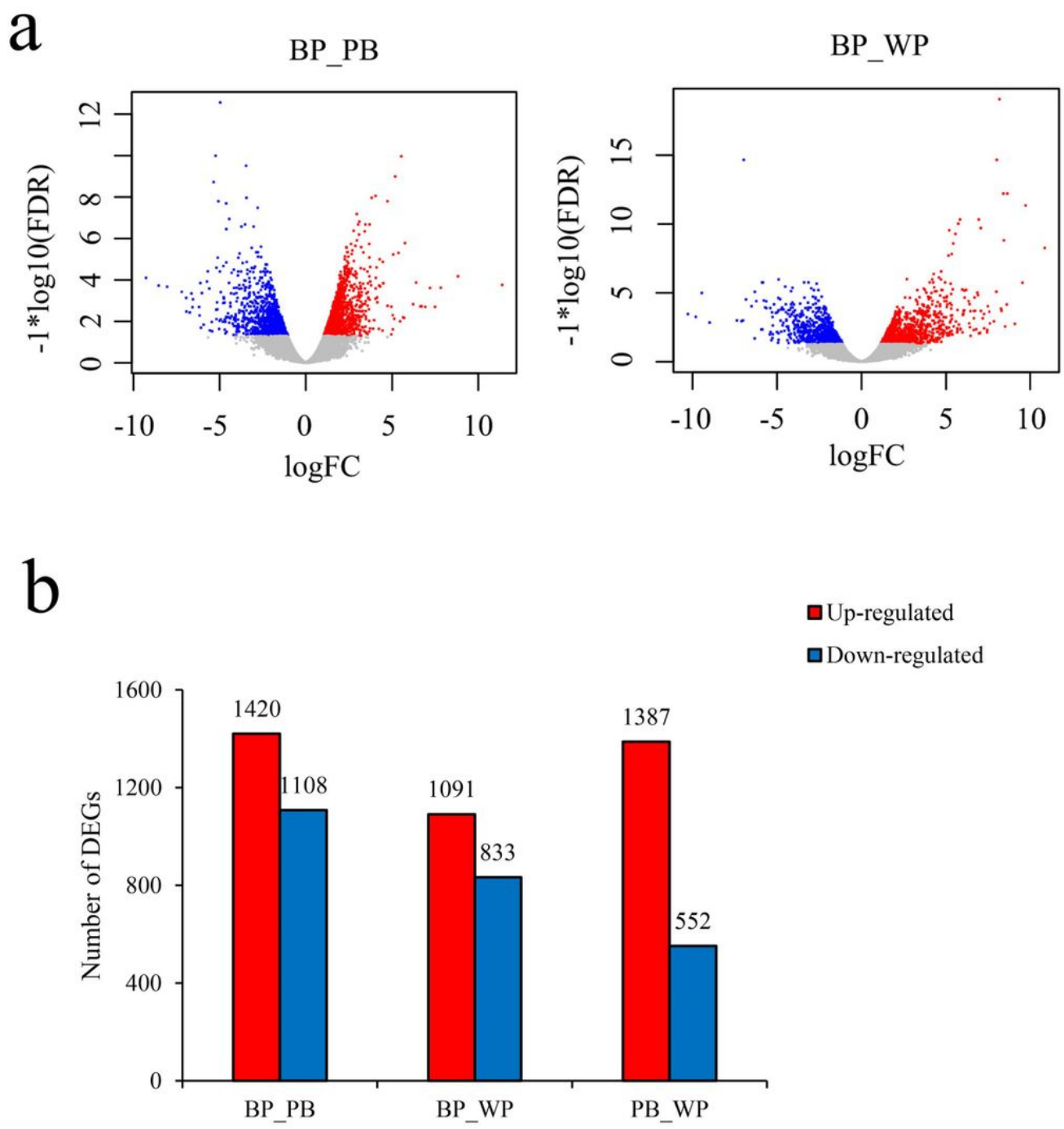

Figure 1

DEGs in BP, WP and PB skins. a, Volcano plot of differential mRNA expression levels among the three pairwise comparisons. The gray, red, and blue dots represent non-significant, up-regulated and down-regulated transcripts, respectively; b, Number of DEGs among the three pairwise comparisons. The red and blue color stand for up-regulated and down-regulated expression, respectively; c, DEGs number and Venn diagram of the overlap of the different groups

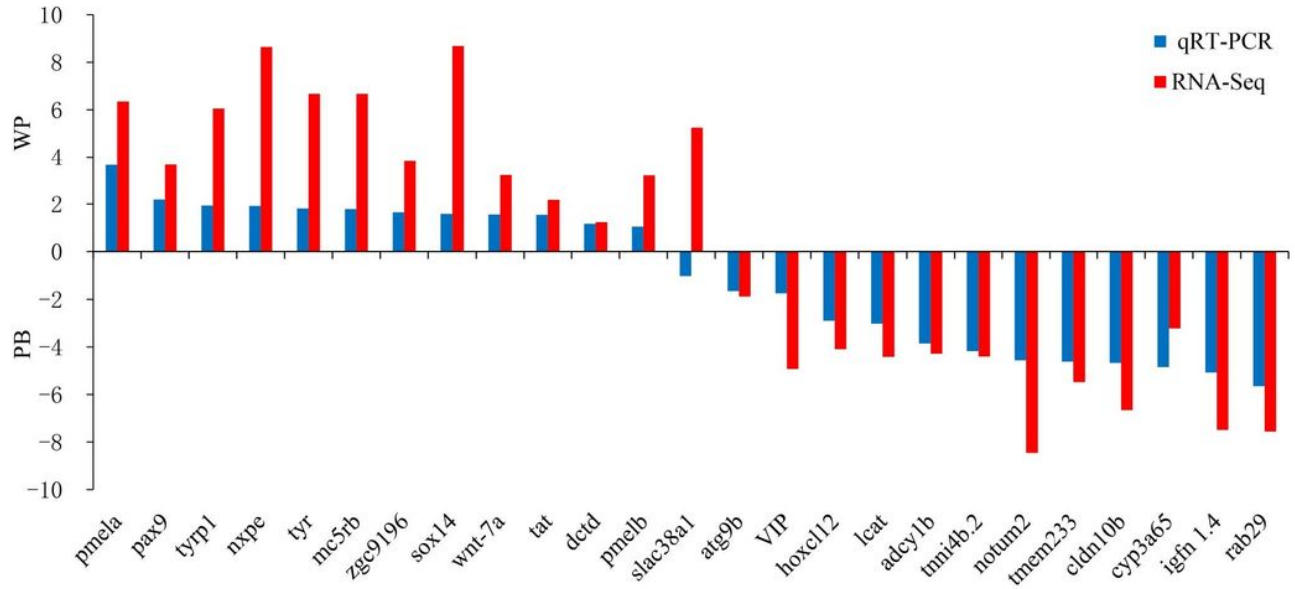

Figure 2

Comparison of mRNA expression levels among the 25 DEGs obtained using qRT-PCR validation and RNA sequencing. Log-fold changes are expressed as the ratio of gene expression after normalization to β-actin

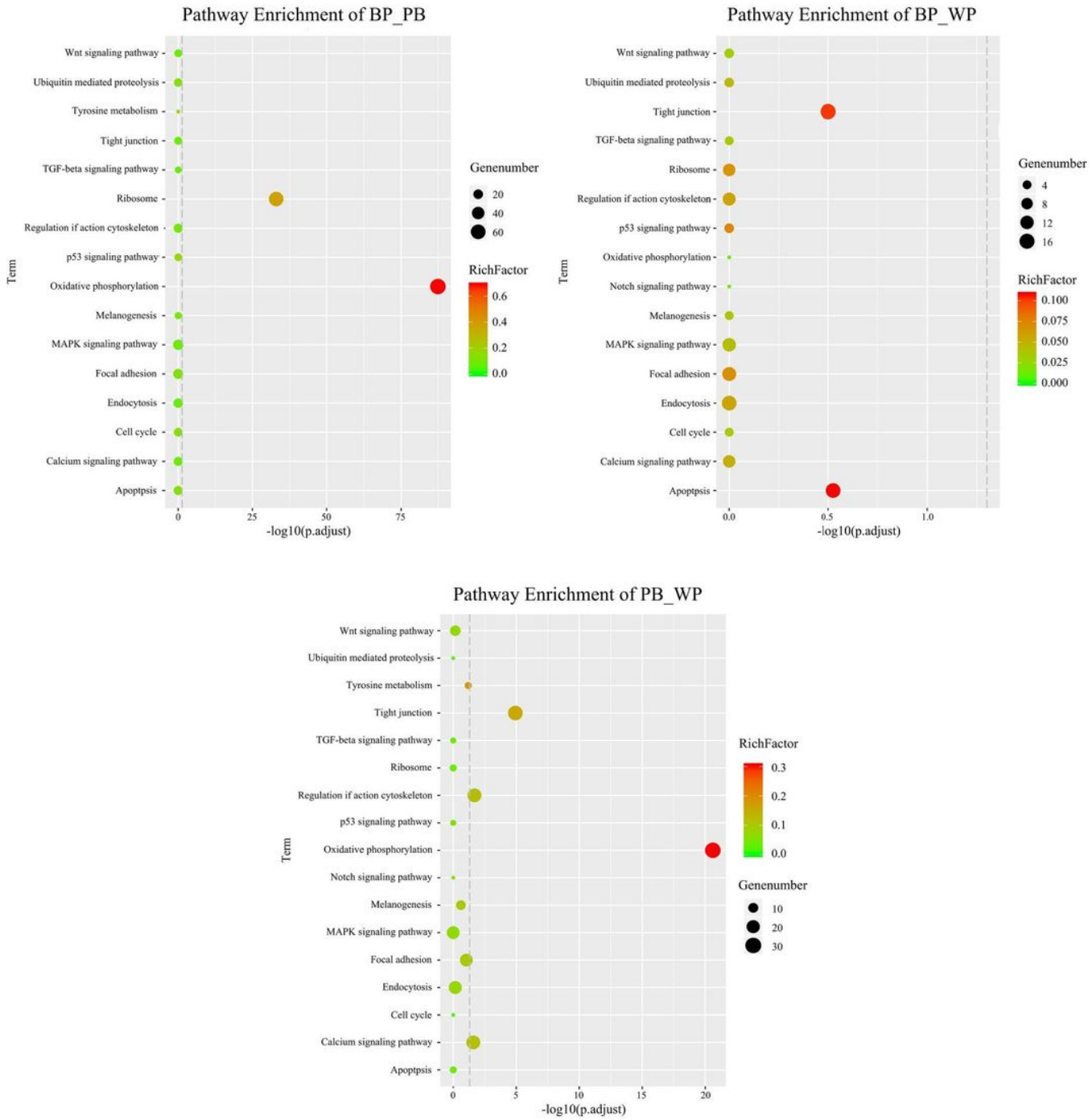

Figure 3

Pigmentation-related pathways based on Kyoto Encyclopedia of Genes and Genomes (KEGG) pathway analysis. Gene number: number of genes in each pathway; Rich factor: ratio of the number of target genes divided by the total number of genes in each pathway

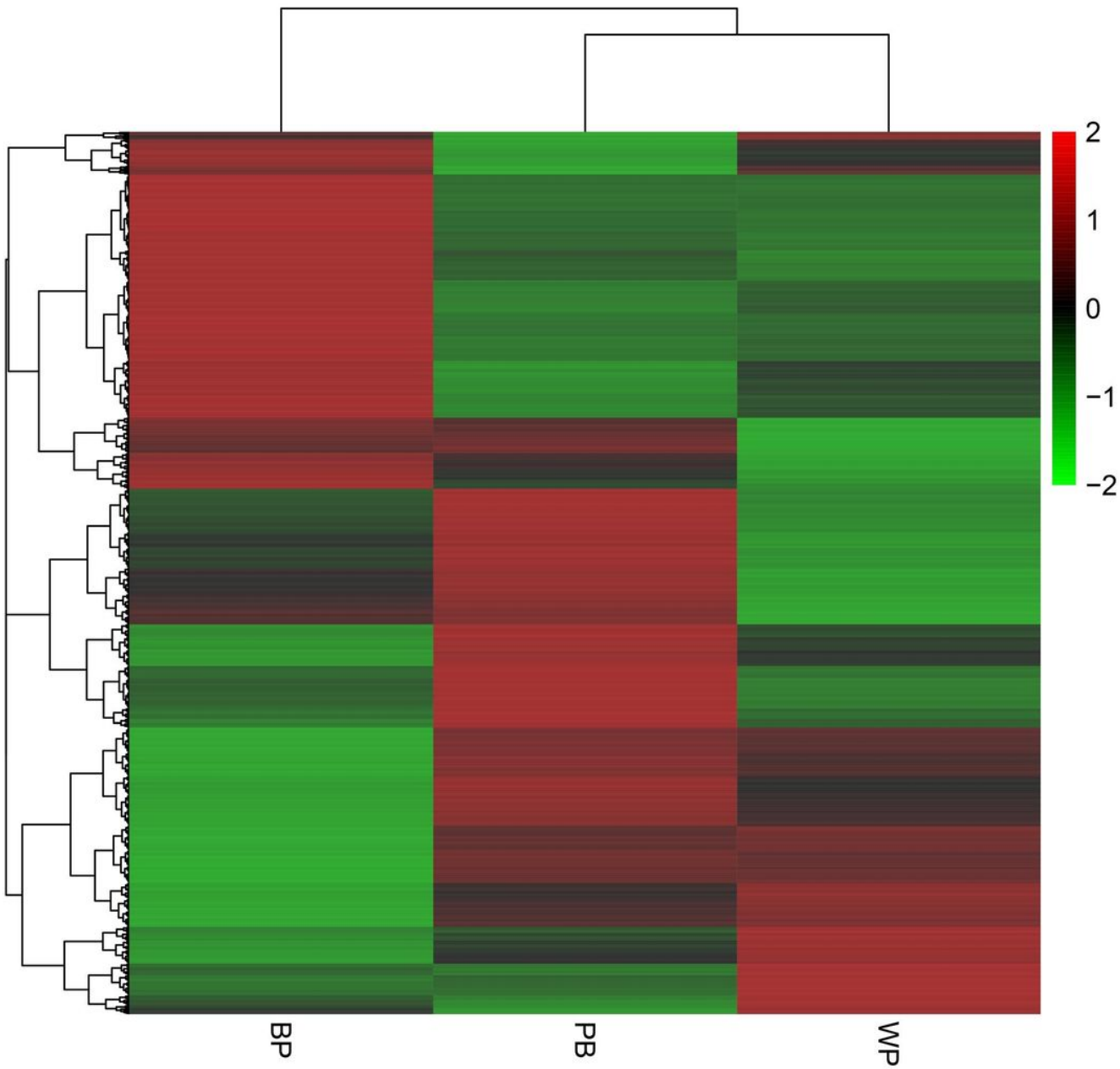

Figure 4

Heatmap of showing the expressions of selected DEGs in WP, PB and BP skins. Note: Each row in the map represents a DEG and column represents condition used; Log10 normalized expression value is used for constructing heat-map

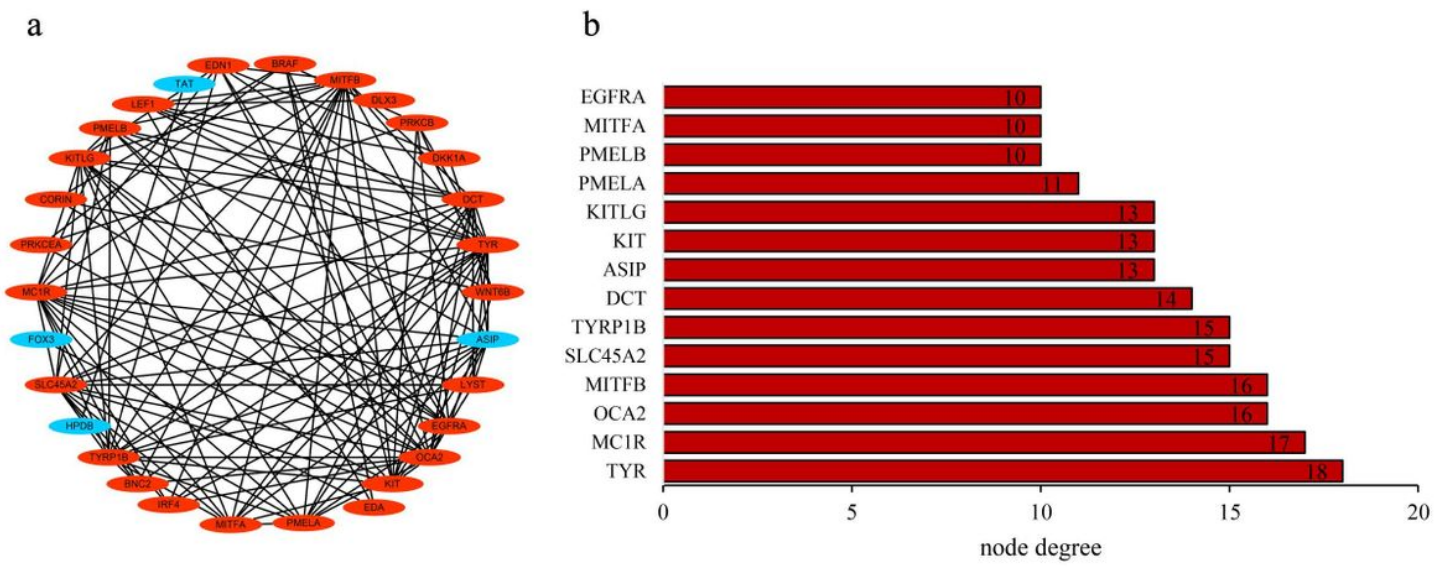

Figure 5

The mutual protein-protein interactions of candidate genes in PB_WP comparison. a, PPI network; b, The genes of the PPI according to the node degree over 10